Heliyon 10 (2024) e27586

Contents lists available at ScienceDirect

Heliyon

journal homepage: www.cell.com/heliyon

Research article

Identifying the tumor-associated macrophage of lung adenocarcinoma reveals immune landscape through omics data integration

Xu Zhang [a], Liwei Wu [b,*], Xiaotian Zhang [c,**], Yanlong Xu [a,***]

[a] Department of Surgery, Jinshan Hospital of Fudan University, Fudan University, Shanghai, PR China
[b] Department of Thoracic Surgery, Shanghai Public Health Clinical Center, Fudan University, Shanghai, PR China
[c] Department of Surgery, Shanghai Fifth People's Hospital, Fudan University, Shanghai, PR China

ARTICLE INFO

Keywords:
Tumor-associated macrophages (TAM)
TUBA1B
PEBP1
Lung adenocarcinoma (LUAD)
Survival
The cancer genome atlas (TCGA)

ABSTRACT

The tumor-associated macrophages (TAM) play a crucial role in lung adenocarcinoma (LUAD), which can cause the proliferation, migration and invasion of tumor cells. In particular, TAMs mainly regulate changes in the tumor microenvironment thereby contributing to tumorigenesis and progression. Recently, an increasing number of studies are using single-cell RNA (Sc-RNA) sequencing to investigate changes in the composition and transcriptomics of the tumor microenvironment. We obtained Sc-RNA sequencing data of LUAD from GEO database and transcriptome data with clinical information of LUAD patients from TCGA database. A group of important genes in the state transition of TAMs was identified by analyzing TAMs at the single-cell level, while 5 TAM-related prognostic genes were obtained by omics data integration, and a prognostic model was constructed. GOBP analysis revealed that TAM-related genes were mainly enriched in tumor-promoting and immunosuppression-related pathways. After ROC analysis, it was found that the AUC of the prognosis model reached 0.751, with well predictive effectiveness. The 5 unique genes, HLA-DMB, HMGN3, ID3, PEBP1, and TUBA1B, was finally identified through synthesized analysis. The transcriptional characteristics of 5 genes were determined through GEPIA2 database and RT-qPCR. The increased expression of TUBA1B in advanced LUAD may serve as a prognostic indicator, while low expression of PEBP1 in LUAD may have the potential to become a therapeutic target.

1. Introduction

Lung cancer incidence rate is increasing worldwide, making it critical in threatening human health [1]. Lung adenocarcinoma (LUAD) accounts for 40–55% of all lung cancers, overtaking lung squamous cell carcinoma (LUSC) as the most common type of lung cancer in many countries [1,2]. Currently, clinical stage is the major method for predicting the prognosis of LUAD. An increasing

* Corresponding author. Department of Thoracic Surgery, Shanghai Public Health Clinical Center, Fudan University Shanghai, Caolang Highway 2901#, Jinshan district, Shanghai, PR China.
** Corresponding author.
*** Corresponding author. Department of Surgery, Jinshan Hospital of Fudan University, Fudan University Shanghai, Longhang Road 1508#, Jinshan district, Shanghai, PR China.
E-mail addresses: docwuliwei@foxmail.com (L. Wu), 1445981826@qq.com (X. Zhang), doctorxyl@163.com (Y. Xu).

https://doi.org/10.1016/j.heliyon.2024.e27586
Received 18 October 2023; Received in revised form 1 March 2024; Accepted 4 March 2024
Available online 10 March 2024

number of studies have found that many heterogeneous cells are present in LUAD tissue [3,4]. These heterogeneous cells comprise the tumor microenvironment that regulates the proliferation, migration, and invasion of LUAD cells [5,6]. In addition, each patient has a unique genetic background. Therefore, due to the several variabilities, clinical stage alone is inaccurate for prognosis of patients with LUAD [7]. Thus, developing a novel prognostic tool based on the gene expression profile of LUAD cells is crucial.

With the development of the sequencing technology, single-cell RNA (Sc-RNA) sequencing has become the major tool for exploring the tumorigenesis and tumor microenvironment and development [8,9]. Sc-RNA sequencing analyzes the biological characteristics of tumors at cellular level. Therefore, Sc-RNA sequencing provides more information than bulk transcriptome sequencing for exploring the detailed mechanisms present in tumors [10].

Numerous immune cells are present in the tumor microenvironment, of which, tumor-associated macrophages (TAMs) are the major components [11,12]. Initially TAMs were assumed to suppress tumor development and activate the immune system [13]. However, recently TAMs have been confirmed to promote tumor development and immunosuppression [14,15]. Therefore, studying the TAMs can help discovering tumor markers and developing novel antitumor drugs.

In this study, a data set of the gene expression in LUAD together with clinical information obtained from The Cancer Genome Atlas (TCGA) and Sc-RNA sequencing data from the Gene Expression Omnibus (GEO) were analyzed. Subsequently, TAM-related genes were screened out. The TAM-related gene signature was identified to predict the survival and prognosis of patients with LUAD. Currently, many studies exist that address TAM in lung adenocarcinoma, which have revealed the heterogeneity of TAM in lung adenocarcinoma [16]. However, few studies have focused on the impact of key TAM-related genes on patient prognosis [17]. These studies also only examined the effect of individual genes on patient prognosis and did not combine genes to construct prognostic models [18]. Therefore, this study provides a prognostic prediction model constructed using TAM-related genes, enabling a more accurate prediction of patient prognosis and paving the way for future research.

2. Materials and methods

2.1. Single-cell RNA sequencing data

The Sc-RNA sequencing data (GSE117570) used in the study were obtained from the GEO database (https://www.ncbi.nlm.nih.gov/geo/). The raw data comprised four early-stage tumor samples of patients with non-small cell lung carcinoma (NSCLC) and four corresponding paraneoplastic samples. The pathological type of the four NSCLC tumor samples was lung adenocarcinoma (LUAD), as confirmed by the data uploader. The raw data were presented as eight gene expression matrixes, which were collated to generate Seurat objects for downstream analysis.

2.2. RNA sequencing and clinical data of patients with LUAD

The transcriptomics and clinical data used in this study were obtained from TCGA (https://cancergenome.nih.gov/) database. The transcriptomic data were collated into a gene expression matrix, and 954 patients with LUAD were identified to conduct further analysis. Ultimately, after normalizing the data (mean 0 and standard deviation 1) and matching the clinical information, 316 patients with LUAD were included in this study. The rearranged gene expression matrix and clinical raw data were used for further analyses.

2.3. Identification of TAMs and immune landscape in LUAD

Analysis was performed using the R package “Seurat” [19]. To remove overexpressed and sequenced oversaturated cells, the expression matrix was filtered following the criteria: nCount_RNA >1000 & nFeature_RNA <5000 & percent.MT < 30 & nFeature_RNA >600. Subsequently, principal component analysis (PCA) and uniform manifold approximation and projection (UMAP) reductions were used to cluster all cells and annotate the clustered cells using cluster marker genes. The TAMs were extracted for PCA and UMAP reductions. The pseudotime analysis was performed using the R package “monocle” [20] to explore the trajectory of the gene changes in TAMs. In addition, the BEAM function was utilized to explore the specific changes of genes in TAMs.

2.4. Construction of TAM-related prognostic model in LUAD

To establish the relationship between TAM-related genes and the prognoses of patients, a univariate feature selection was conducted. The genes initially screened using the univariate feature selection were screened again using the multivariate feature selection. For both screening analyses a p-value <0.01 was considered statistically significant [21,22]. Subsequently, we performed a third screening of the obtained prognosis-related genes using Kaplan–Meier analysis and finally identified the prognosis-associated TAM-related genes. The prognosis-associated TAM-related genes were used to construct a prognostic model, and the risk score was calculated using the formula [23]:

$$Riskscore = \sum_{i=0}^{n} coef(RNAi) \times expr(RNAi)$$

$coef(RNAi)$ was defined as the coefficient of RNA correlated with survival.
$expr(RNAi)$ was defined as the RNA expression.
The patients with LUAD were divided into high-risk and low-risk groups based on median risk scores. The Kaplan–Meier survival

analysis was performed to estimate the survival difference between the two groups. We used the R package "survival" to conduct this analysis.

2.5. The effect evaluation of the TAM-related gene prognostic model

To assess the effectiveness of risk scores, univariate and multivariate Cox regression analyses were performed to comprehensively evaluate the relationship between the model and survival of patients with LUAD. The time-dependent receiver operating characteristic (ROC) curve was used to evaluate the predictive ability of the model and the area under the curve (AUC) was calculated to quantify the predictive ability. We used R package "survival" and R package "survivalROC" to perform these analyses.

2.6. Acquisition of lung cancer and paracancer tissues

Lung tissue was collected after the resection of lung cancer and divided into paracancer and lung cancer tissues. To extract total RNA, the tissues were placed into the labeled centrifuge tubes and stored at −80 °C. Informed consent from patients were obtained prior to the surgeries, and all experimentation procedures were reviewed and approved by the Ethics Committee of the Jinshan Hospital (JIEC 2022-S56). A total of 18 samples from nine patients with LUAD were collected for RNA and protein extractions. The clinical data of the nine patients with LUAD are shown in Table 1.

2.7. Real-time quantitative polymerase chain reaction (RT-qPCR)

The total RNA was extracted from the tissues using an RNA extraction kit (no. R701-01, Vazyme) following the manufacturer's instructions. Reverse transcription was performed using a Primescript RT reagent kit (no. RR047Q, Takara) and the Life Technology ABI 7500 System based on SYBR-Green PCR kit (no. A25742, Thermo Fisher Scientific). The $^{\triangle\triangle}$Ct method was used for calculating the gene expression relative to a housekeeping gene. The primer sequences used in the RT-qPCR are presented in Table 2.

2.8. Western blotting

Total protein was extracted from the tissue samples using radioimmunoprecipitation assay (RIPA) buffer (no. P0013B, Beyotime) following the manufacturer's instructions. Ten micrograms of protein were loaded into a 4–12% Bis-Tris gel (no. NW04120BOX, Thermo Fisher Scientific) and subjected to electrophoresis at 80 V for 0.5 h and then 120 V for 1.5 h. Subsequently, the proteins were transferred to a nitrocellulose membrane (no. IB33002, Thermo Fisher Scientific) for 6 min at 48 V. The membrane was incubated with 5% milk in Tris-buffered saline with 0.1% Tween® 20 detergent (TBST) for 1 h to block non-specific antibody binding. Membranes were then incubated with the primary antibodies in TBST overnight at 4 °C. The primary antibodies used in this study were: TUBA1B (no. ab108629, Abcam, 1:2000), PEBP1 (no. ab76582, Abcam, 1:2000), and GAPDH (no. ab181602, Abcam, 1:2000). Subsequently, the membranes were washed with TBST for 45 min and incubated with the appropriate horseradish peroxidase (HRP)-conjugated secondary antibody (no. A0208, Beyotime, 1:8000) for 2h. After incubating with the secondary antibody, the membranes were washed with TBST for 45 min. Optical density was determined via densitometry analysis using the ImageJ software.

2.9. Statistical analysis

The R software (version 4.2.2) was used to conduct all analysis. The function annotation was performed using the metascape database (https://metascape.org) and visualized using the R package "ggplot2" [24]. The GEPIA2 database (http://gepia2.cancer-pku.cn/) was used to explore transcription characteristics of the genes of interest [25]. The Prism 9 was used to analyze data from the

Table 1
Clinical data of the nine patients with LUAD that participated in this study.

Age (years)	Sex	Stage	T	M	N
74	Female	Stage IB	T2	M0	N0
65	Male	Stage IB	T2	M0	N0
46	Male	Stage IIA	T2a	M0	N1
69	Male	Stage IIA	T2b	M0	N0
70	Male	Stage IA	T2	M0	N0
74	Female	Stage IIIA	T2	M0	N2
74	Female	Stage IB	T2	M0	N0
74	Male	Stage IA	T1a	M0	N0
73	Male	Stage IIB	T3	M0	N0

Notes: The TNM cancer staging system includes: T, extent of the tumor (T1a, extent of the tumor≤1 cm; T2, 3 cm < extent of the tumor≤5 cm; T2a, 3 cm < extent of the tumor≤4 cm; T2b, 4 cm < extent of the tumor≤5 cm; T3, 5 cm < extent of the tumor≤7 cm); M, presence of metastasis (M0, no presence of metastasis); and N, lymph nodes (N0, no regional lymph node metastasis; N1, metastasis in ipsilateral peribronchial and/or ipsilateral hilar lymph nodes and intrapulmonary nodes, including involvement by direct extension; N2, metastasis in ipsilateral mediastinal and/or subcarinal lymph nodes).

Table 2
Primer sequences used in the real-time polymerase chain reaction.

Genes	Forward primer	Reverse primer
HLA-DMB	TGGGGTGCTGAATAGCTTGG	GGGTGTGTGTGGCACAATTC
HMGN3	CAGAGAATACAGAGGGCAAAGATGG	CAGTTTTCTGTGCCTCTTCAGC
ID3	AGCGCGTCATCGACTACATT	TGACAAGTTCCGGAGTGAGC
PEBP1	CGCCCACCCAGGTTAAGAAT	GGTCTGTCAGGACCAAGGTG
TUBA1B	CAACTACCAGCCTCCCACTG	CATGCTGCAGGGCCAAAAG

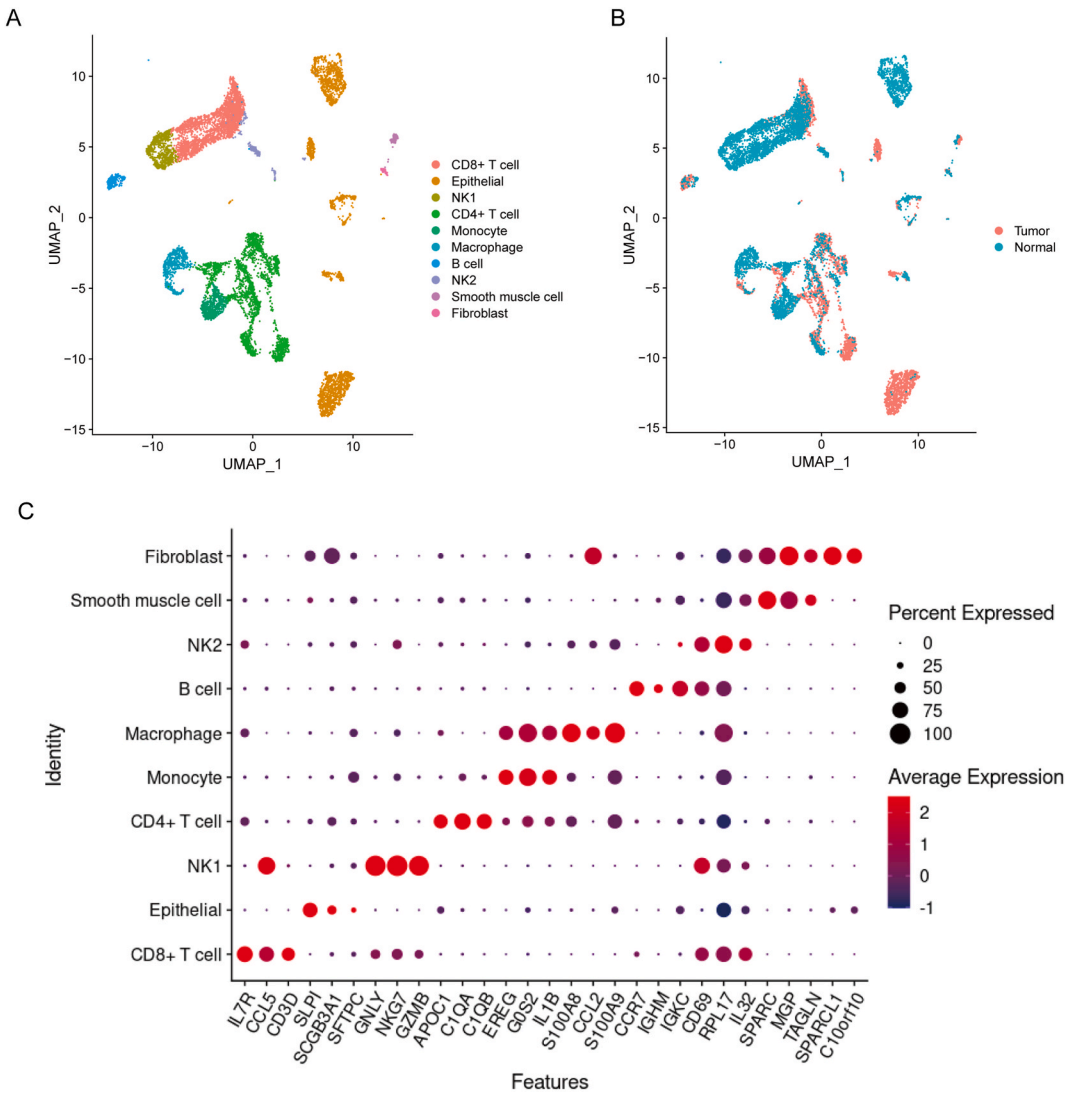

Fig. 1. The atlas of LUAD at single cell level resolution. A, the cell type clusters of LUAD. B, the group clusters of LUAD. C, the marker genes of cell type clusters, and the red dot represents high level of average expression, while blue dot represents low level of average expression, besides, the size of dot represents percentage of cells expressing the marker. (For interpretation of the references to colour in this figure legend, the reader is referred to the Web version of this article.)

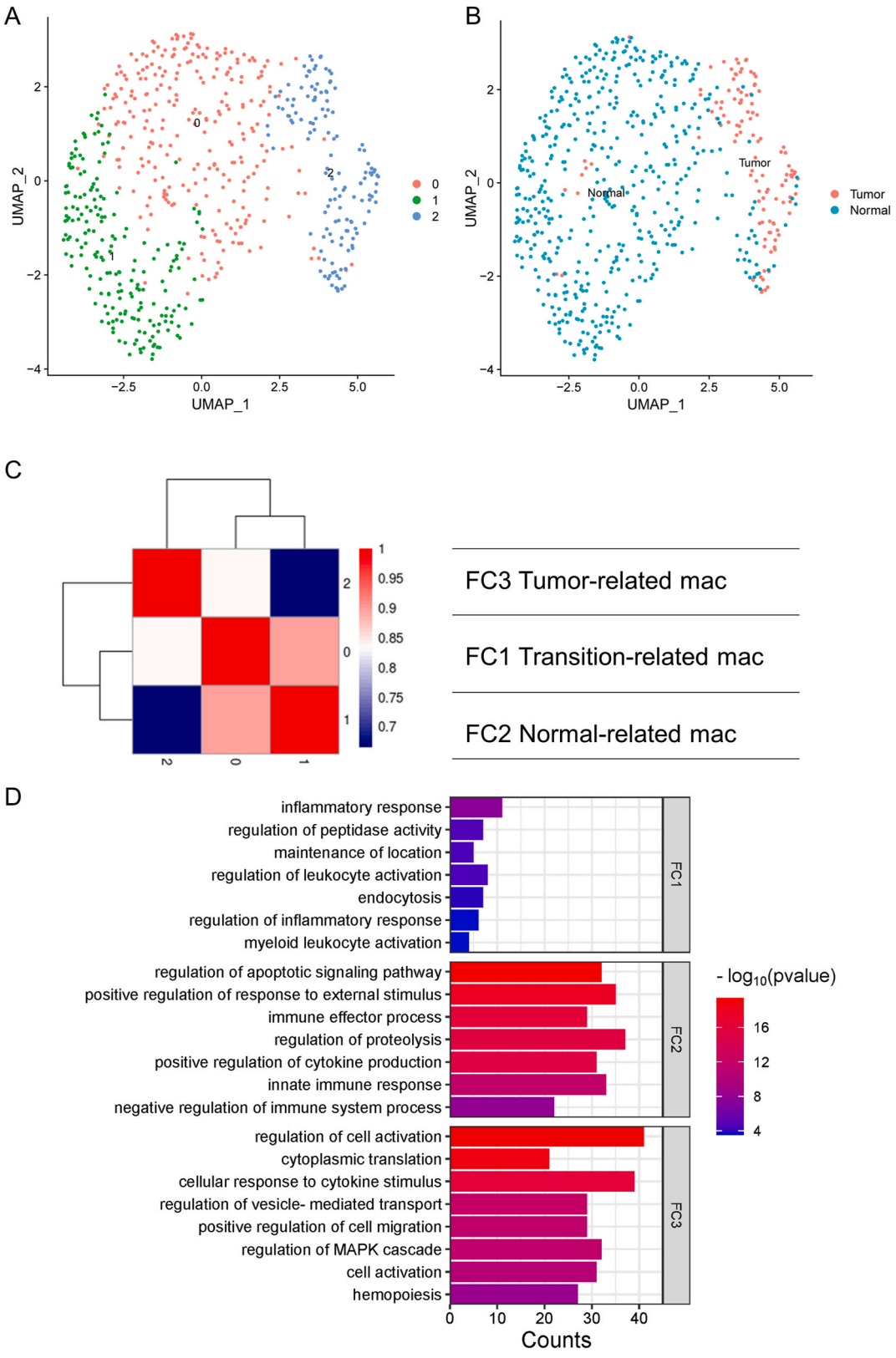

(caption on next page)

Fig. 2. The comprehensive analysis of macrophages of LUAD at single cell level resolution. A, the Seurat clusters of macrophages. B, the group clusters of macrophages. C, the markable gene average expression heatmap of Seurat clusters of macrophages, and the red square represents high level of Pearson correlation coefficient, while blue square represents low level of Pearson correlation coefficient. D, the GOBP enrichment of marker genes of macrophages, and red bar represents low level of *P*-value, while blue bar represents high level of *P*-value, besides, the length of bar represents gene counts in each GOBP term. (For interpretation of the references to colour in this figure legend, the reader is referred to the Web version of this article.)

RT-qPCR and Western blotting. The student *t*-test was used to evaluate the statistical significance and $P < 0.05$ was considered statistically significant.

3. Results

3.1. Sc-RNA atlas of LUAD

The Sc-RNA sequencing data were filtered and 10,408 cells were retained for subsequent analysis. After UMAP reduction, the cells were classified into 22 clusters, which were annotated using marker genes. Finally, 10 clusters were identified using the CellMarker database (http://xteam.xbio.top/CellMarker/), most of which were immune cells (Fig. 1A), indicating that immune cells play a crucial role in early tumorigenesis and LUAD development. A high heterogeneity between LUAD and normal lung tissues (Fig. 1B) was observed, revealing the changes in the biological functions of various cells in tumor tissues, contributing to the formation of a tumor microenvironment with the conditions necessary for tumorigenesis. We also obtained the results of cell annotation and visualized the marker genes for each cell type using dot plots (Fig. 1C).

3.2. Identification of specific LUAD TAMs

The UMAP reduction was used to analyze the heterogeneity among macrophages and three clusters of macrophages were identified (Fig. 2A). A total of 601 macrophages were extracted for analysis, of which, 484 macrophages were from normal lung tissues and 116 macrophages were from tumor tissues (Fig. 2B). The gene expression patterns of the three macrophages clusters differed from each other. Therefore, the macrophages were categorized into three different functional subtypes (Fig. 2C). The Gene Oncology Biological Process (GOBP) annotation of the marker genes of the functional subtypes revealed that FC1 macrophages were mainly responsible for immune response, whereas FC2 macrophages were primarily responsible for immunomodulation, and the FC3 macrophages were chiefly involved in the tumor immunity-related functions (Fig. 2D). The cells of FC2 were mainly derived from normal lung tissues, whereas the cells of FC3 were primarily derived from tumor tissues. The large functional difference between FC2 and FC3 in the GOBP analysis illustrates the high heterogeneity of macrophages in normal lung and tumor tissues.

3.3. Pseudotime analysis of LUAD macrophages

The 601 macrophages were arranged on a trajectory distribution map based on the degree of genetic change, which demonstrated that a more pronounced conversion of macrophages from a normal to a tumor state occur (Fig. 3A). The left side of the trajectory was almost exclusively composed of macrophages from the normal lung tissue, whereas the right side had an increased percentage of macrophages from the tumor tissue, and the bottom side had macrophages from both normal lung and tumor tissues. After replacing the cell labels, FC1 macrophages were observed to be in the transition state mainly, FC2 macrophages were primarily in the normal state, and FC3 macrophages were chiefly in the tumor state, which is consistent with the function subtypes identified by the gene expression patterns (Fig. 3B). The gene enrichment analysis of normal, tumor, and transition states revealed gene expression differences between the three states. A strong immune activation was observed in macrophages in the tumor state. Contrarily, the activation of metabolism-related pathways in macrophages was in the normal state, and that of the glucose metabolism-related pathways in macrophages was in the transformed state (Fig. 3C). All macrophage-related genes were categorized into three clusters based on their expression patterns. The genes in cluster 1 were more expressed in the transition and normal states, in cluster 2 were more expressed in the tumor state, and in cluster 3 were more expressed in the transition state (Fig. 3C). Thus, we selected the genes enriched in cluster 2 (with higher expression in tumor state) to explore the prognostic value.

3.4. Construction of a TAM-related gene prognostic model in LUAD

A total of 121 genes in cluster 2 were obtained using the BEAM function. Furthermore, the univariate Cox proportional hazard analysis identified 28 prognostic genes from 121 genes ($P < 0.01$), including 18 high-risk genes ($HR > 1$) and 10 low-risk genes ($HR < 1$). Subsequently, the multivariate Cox proportional hazard analysis identified five survival-associated genes from 28 prognostic genes ($P < 0.01$). The five genes associated to survival were: *HLA-DMB*, *HMGN3*, *ID3*, *PEBP1*, and *TUBA1B*. The five survival-associated genes were used to construct a TAM-related gene prognostic model [risk score = (0.005 × TUBA1B) + (0.028 × HLA-DMB) + (−0.004 × PEBP1) + (0.003 × HMGN3) + (0.009 × ID3)].

Patients with LUAD were divided into high- and low-expression groups based on the median expression of the five survival-associated genes. The overall survival (OS) was significantly different ($P < 0.05$) (Fig. 4A–E). Based on the risk score calculated

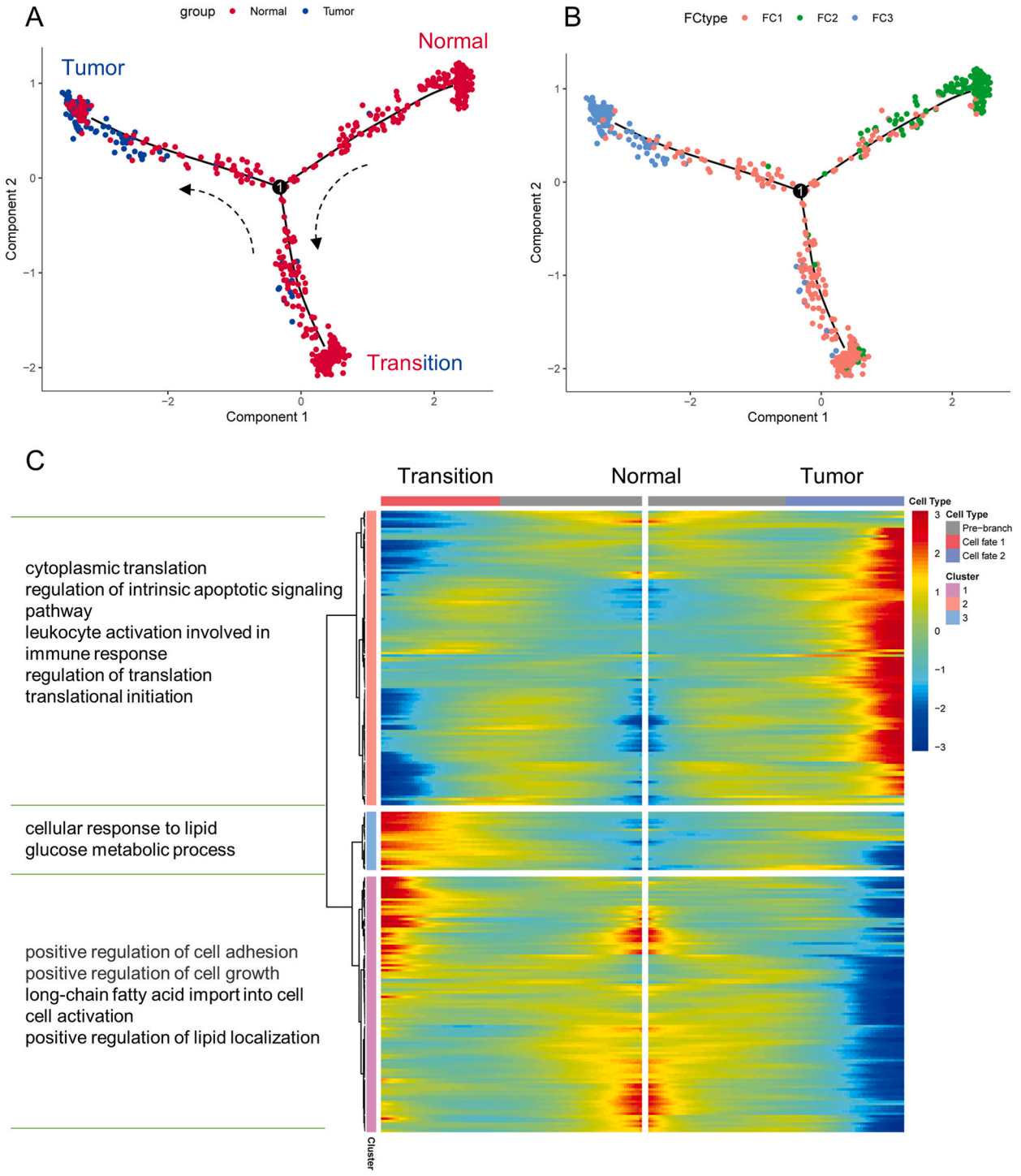

Fig. 3. The pseudotime analysis of macrophages of LUAD. A, the trajectory map of macrophages of LUAD in group types. B, the trajectory map of macrophages of LUAD in function subtypes. C, the BEAM heatmap of macrophages, and the GOBP enrichment of genes in 3 clusters located left side, besides, the red point represents high expression of gene while blue point represents low expression of gene. (For interpretation of the references to colour in this figure legend, the reader is referred to the Web version of this article.)

using formula 1, we divided the patients with LUAD into high- and low-risk groups according to the median of risk score. The OS was statistically significant ($P < 0.01$) (Fig. 5A). The risk score and the relevant survival statuses of the patients with LUAD were observed using the risk curve and scatterplot (Fig. 5C and D), indicating that the mortality was associated with the risk score. The heatmap of the

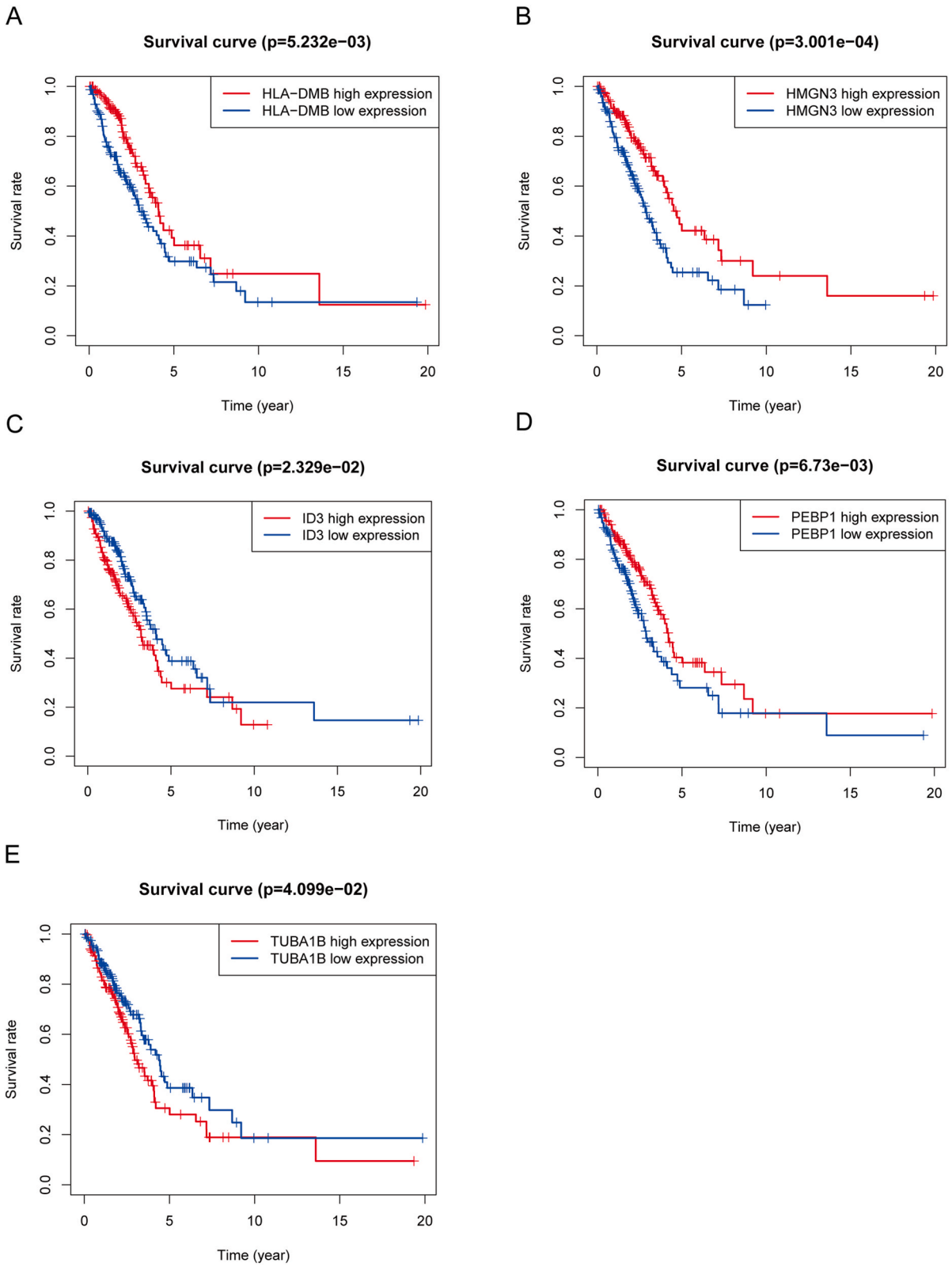

Fig. 4. The survival curve of 5 TAM-related genes. A, the survival curve of HLA-DMB. B, the survival curve of HMGN3. C, the survival curve of ID3. D, the survival curve of PEBP1. E, the survival curve of TUBA1B.

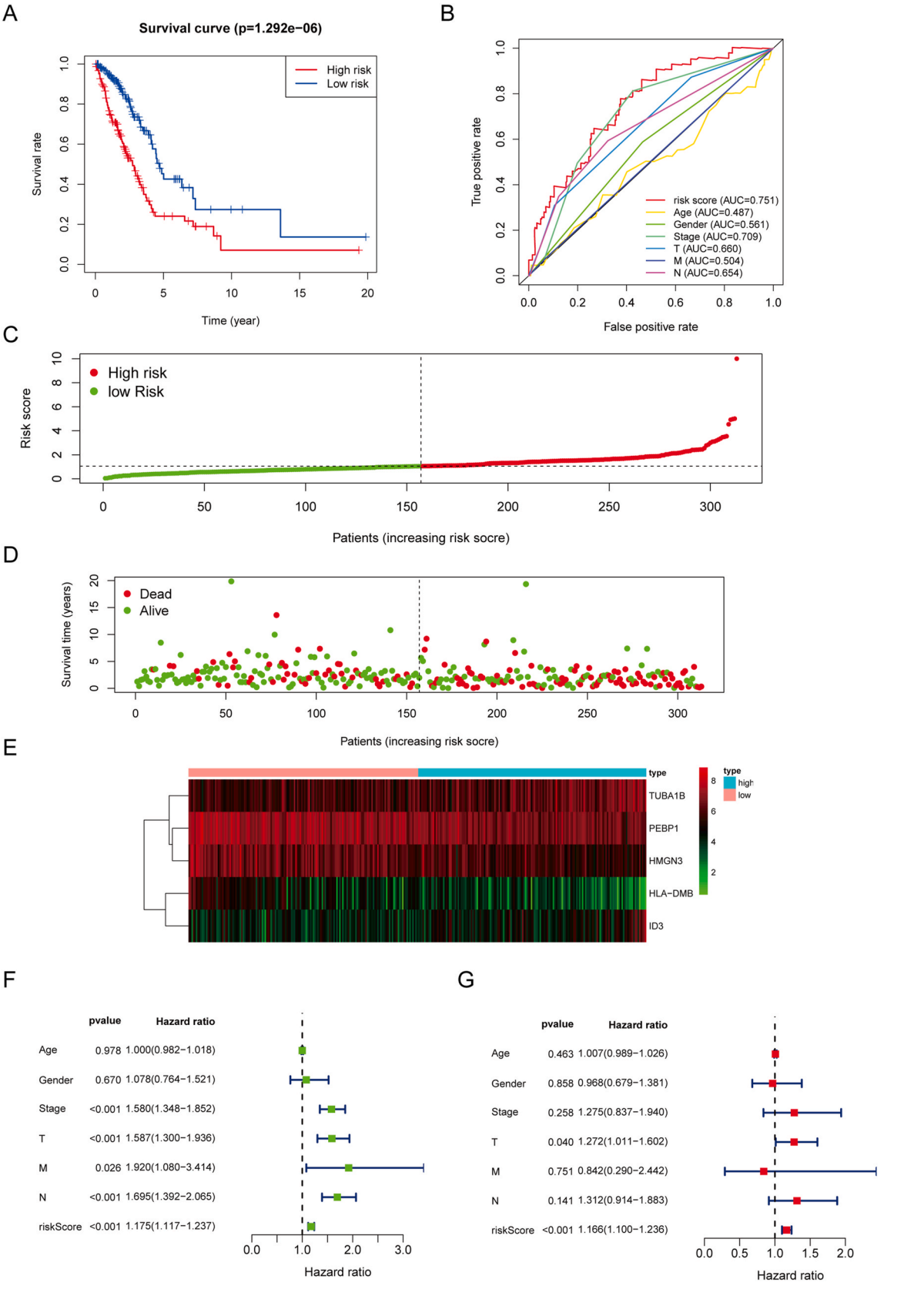

(caption on next page)

Fig. 5. The comprehensive validation of risk score. A, the survival curve of risk score. B, the ROC curve of risk score. C, the risk curve based on the risk score of each sample. D, the scatterplot based on the survival status of each sample, and the green and red dots represent survival and death. E, the heatmap displayed the expression levels of TAM-related genes in the high-risk and low-risk groups. F, the results of univariate Cox regression analysis of risk score and other clinical factors. G, the results of multivariate Cox regression analysis of risk score and other clinical factors. Clinical factors: age, gender, stage, T (tumor size), N (lymph node metastasis) and M (distant metastasis). (For interpretation of the references to colour in this figure legend, the reader is referred to the Web version of this article.)

five TAM-related genes revealed the expression profile characteristics of the genes in patients with LUAD (Fig. 5E).

To assess whether the risk score was an independent prognostic factor for the patients with LUAD, we performed univariate and multivariate Cox regression analyses. The hazard ratio (HR) of the risk score was 1.175 (95% confidence interval (CI): 1.117–1.237) ($P < 0.01$) in the univariate Cox regression analysis (Fig. 5F). In contrast, the HR of the risk score was 1.166 (95% CI: 1.100–1.236) ($P < 0.01$) in the multivariate Cox regression analysis (Fig. 5G). Therefore, the risk score can be an independent prognostic factor for patients with LUAD. The AUC of the risk score was 0.751, which was the highest among other clinical factors, indicating that risk score can be used as a predictor for the prognosis of patients with LUAD (Fig. 5B).

3.5. Cross-validation of five TAM-related genes

We noticed that five TAM-related genes had prognostic value, which was displayed as the Kaplan–Meier survival plots. The GEPIA2 database was used to explore the transcription characteristics of the five TAM-related genes. This analysis demonstrated that *HMGN3* and *TUBA1B* had different expression patterns among the four stages (Fig. 6B and E); however, *HLA-DMB*, *ID3*, and *PEBP1* had no differences in the expression pattern among the four stages (Fig. 6A, C, and 6D). Moreover, the stage IV patients with LUAD had highest *TUBA1B* expression level, indicating that *TUBA1B* might be related to the progression of stage IV lung cancer. The RT-qPCR and WB indicated that expression level of *PEBP1* was lower in the LUAD lung tissue than that in paracancer tissue (Fig. 6I, K and 6L). In addition, *TUBA1B* was higher in LUAD lung tissue than that in paracancer tissue (Fig. 6J, K and 6M) ($P < 0.05$). In contrast, *HLA-DMB*, *HMGN3,* and *ID3* had no statistically significant differences between the paracancer and LUAD lung tissues (Fig. 6F, G, and 6H).

4. Discussion

Lung cancer can be classified into small cell lung cancer and non-small cell lung cancer based on pathomorphological manifestations [26]. Among them, LUSC and LUAD account for the highest incidence rate of non-small cell lung cancer [26,27]. The LUAD incidence rate is increasing annually and exceeded the incidence rate of LUSC(26). Currently, LUAD is a relevant medical issue that needs urgent attention and solution. Compared with LUSC, LUAD is more closely related to post-transcriptional regulation [28–30]. Therefore, exploring the transcriptomics of LUAD is crucial. Recently, Sc-RNA sequencing has become a powerful tool for exploring the tumor microenvironment. Sc-RNA sequencing analyzes the tumor tissue at cellular level, thus providing more information than the bulk transcriptome sequencing.

Many immune cells are present in the tumor microenvironment, which play a crucial role in tumor development [31]. Among these immune cells, TAMs are the most prominent components [31]. TAMs promote tumorigenesis and tumor development via multiple cellular pathways [32,33]. Therefore, exploring the transcriptomics of TAMs can help to develop more sensitive tumor markers and therapeutic targets. In this study, we identified genes closely related to tumorigenesis by investigating genes that undergo expression pattern shifts in the state transitions of TAMs. Using survival analysis, we identified five genes that may serve as tumor markers and therapeutic targets.

The results of the univariate Cox regression analysis revealed that the risk score can be used as an independent prognostic factor and a prognosis tool for the patients with LUAD as other clinical indicators [23]. The results of the multivariate Cox regression analysis further confirmed this finding. Currently, the stage system of LUAD is frequently used to predict the prognosis of patient in the clinical practice. However, single-cell sequencing studies on LUAD have revealed that LUAD tissue comprises cancer cells and various heterogeneous cells that collectively constitute the tumor microenvironment. These cells impact the proliferation, migration, and invasion of cancer cells [34,35]. Therefore, simply using the stage system of LUAD for prognosis is inaccurate. The genetic background and tumor microenvironment of each patient are different; thus, even patients with the same cancer stage have different prognosis. Consequently, developing prognosis prediction models based on transcriptomics is important.

In the ROC, the AUC of the risk score reached 0.751, whereas the AUC of the clinical stage was only 0.709, which further demonstrates the accuracy of the prognosis model. GOBP analysis indicated that functions of cluster 2 and FC3 genes were majorly enriched in tumor-promoting and immunosuppression-related pathways. Among these functions the cell activation, positive regulation of cell migration, and regulation of MAP Kinase (MAPK) cascade were enriched mostly. Four classes of MAPK pathways are known, among which the Ras/Raf/MEK/ERK pathway is the most closely related to tumorigenesis and cancer development [36]. The function of TAMs is closely related to the activation of the MAPK pathway. The MAPK pathway regulates the biological pattern of epithelial cells by autocrine and paracrine regulation of the ligand expression in the tumor microenvironment, thereby generating proliferation- and migration-related secondary signaling to malignant epithelial cells.

The RT-qPCR and Western blotting analyses showed that *TUBA1B* and *PEBP1* were differentially expressed in tumor and paracancer tissues. *TUBA1B* has not been well studied; however, it is predicted to be involved in microtubule cytoskeleton organization and mitotic cell cycle, and to act upstream of or within cellular response to interleukin-4. *TUBA1B* expression in tumors leads to poor

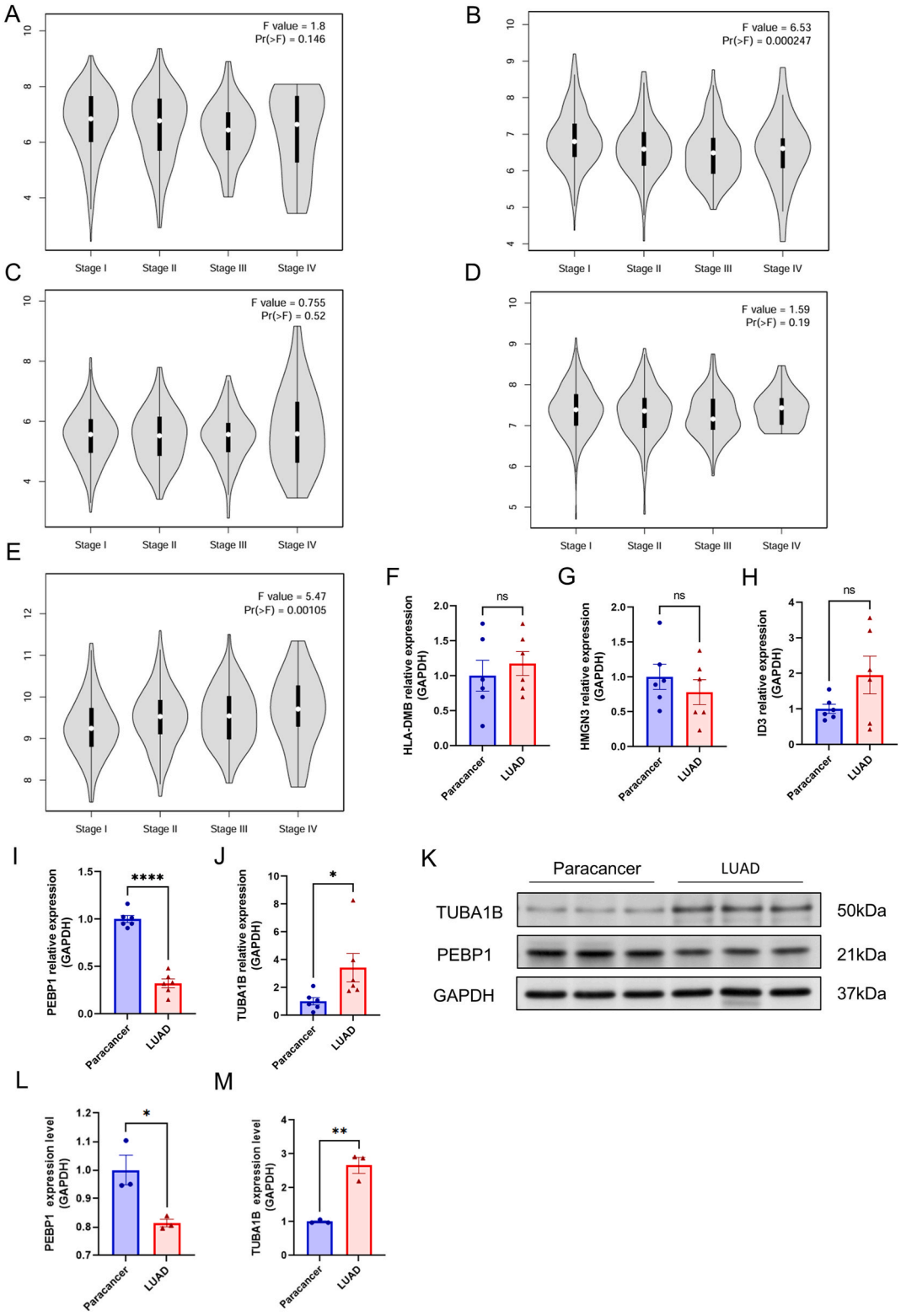

(caption on next page)

Fig. 6. The cross validation of 5 TAM-related genes. A, the stage expression level of HLA-DMB. B, the stage expression level of HMGN3. C, the stage expression level of ID3. D, the stage expression level of PEBP1. E, the stage expression level of TUBA1B. F, the RT-qPCR of HLA-DMB. G, the RT-qPCR of HMGN3. H, the RT-qPCR of ID3. I, the RT-qPCR of PEBP1. J, the RT-qPCR of TUBA1B. K, the Western blot of PEBP1 and TUBA1B. L, the statistic analysis of WB in PEBP1. M, the statistic analysis of WB in TUBA1B. "*" represents *P*-value <0.05; "**" represents *P*-value <0.01; "***" represents *P*-value <0.001; "****" represents *P*-value <0.0001.

prognosis and chemoresistance [37,38]; however, its exact mechanism remains unexplored. In this study, using single-cell data, we observed that *TUBA1B* was highly expressed in TAMs, and an indirect regulatory mechanism to control the biological characteristics of tumor cells may exist. The data of GEPIA2 showed that the expression of *TUBA1B* increased significantly in LUAD stage IV. That is, *TUBA1B* is not expressed at high levels in tumor cells to promote tumor development, rather, it is expressed at high levels in TAMs to promote changes in the tumor microenvironment, thereby enabling tumor proliferation and metastasis.

PEBP1 encodes a member of the phosphatidylethanolamine-binding family of proteins and has been shown to modulate multiple signaling pathways, including the MAPK, NF-kappa B, and glycogen synthase kinase-3 (GSK-3) signaling pathways [39]. PEBP1 plays a key role in various tumors, mainly by inhibiting tumor metastasis [40,41]. Conversely, data from GEPIA2 showed that the *PEBP1* expression did not differ significantly in any of the four stages of tumorigenesis and cancer development. Although, the major mechanisms by which *PEBP1* functions have been explored in many studies, in this study *PEBP1* was expressed in tumor-associated macrophages, providing another perspective for the study of the tumor microenvironment in LUAD.

This study had some limitations. First, the specific regulatory mechanisms and therapeutic strategies of *TUBA1B* and *PEBP1* in LUAD had not been thoroughly investigated. Second, the established prognosis model requires external validation with a large amount of data. Third, other prognostic TAM-related genes in the prognosis model requires more in-depth mechanism research. Finally, we used only one single-cell data for our analysis, therefore, the results may not be comprehensive. This study indicates the direction for future research on TAMs in LUAD. In future research, we will focus on exploring the biological mechanisms of TAMs in LUAD and developing novel therapeutic strategies.

5. Conclusion

In conclusion, we identified a novel TAM-related prognostic model consisting of five genes (*HLA-DMB, HMGN3, ID3, PEBP1,* and *TUBA1B*) in LUAD. The increased expression of *TUBA1B* in advanced LUAD may be a prognostic marker; in contrast, the low expression of *PEBP1* in LUAD indicates that *PEBP1* can potentially be a therapeutic target. These findings pave the way for future research on LUAD treatment.

Ethics approval and consent to participate

The ethics of this study was approved by the Ethics Committee of Jinshan Hospital (JIEC 2022-S56). Each patient participating in the study signed an informed consent.

Consent for publication

Not applicable.

Data availability statement

All data used in this study were acquired from The Cancer Genome Atlas (TCGA) portal and GEO database (GSE117570).

Funding

Not applicable.

CRediT authorship contribution statement

Xu Zhang: Writing – original draft, Methodology. **Liwei Wu:** Writing – review & editing, Supervision, Methodology, Formal analysis. **Xiaotian Zhang:** Writing – review & editing, Writing – original draft. **Yanlong Xu:** Writing – review & editing, Supervision, Methodology.

Declaration of competing interest

The authors declare that they have no known competing financial interests or personal relationships that could have appeared to influence the work reported in this paper.

Acknowledgements

Not applicable.

Appendix A. Supplementary data

Supplementary data to this article can be found online at https://doi.org/10.1016/j.heliyon.2024.e27586.

References

[1] R. Siegel, K. Miller, N. Wagle, A. Jemal, Cancer statistics, 2023, CA A Cancer J. Clin. 73 (1) (2023) 17–48, https://doi.org/10.3322/caac.21763.Cited, in: Pubmed; PMID 36633525.
[2] N. Vokes, K. Pan, X. Le, Efficacy of immunotherapy in oncogene-driven non-small-cell lung cancer, Therapeutic advances in medical oncology 15 (2023) 17588359231161409, https://doi.org/10.1177/17588359231161409.Cited in: Pubmed; PMID 36950275.
[3] Q. Yang, H. Zhang, T. Wei, et al., Single-cell RNA sequencing reveals the heterogeneity of tumor-associated macrophage in non-small cell lung cancer and differences between sexes, Front. Immunol. 12 (2021) 756722, https://doi.org/10.3389/fimmu.2021.756722. . Cited in: Pubmed; PMID 34804043.
[4] F. Wu, J. Fan, Y. He, et al., Single-cell profiling of tumor heterogeneity and the microenvironment in advanced non-small cell lung cancer, Nat. Commun. 12 (1) (2021) 2540, https://doi.org/10.1038/s41467-021-22801-0. Cited in: Pubmed; PMID 33953163.
[5] N. Altorki, G. Markowitz, D. Gao, et al., The lung microenvironment: an important regulator of tumour growth and metastasis, Nat. Rev. Cancer 19 (1) (2019) 9–31, https://doi.org/10.1038/s41568-018-0081-9. Cited in: Pubmed; PMID 30532012.
[6] C. Genova, C. Dellepiane, P. Carrega, et al., Therapeutic implications of tumor microenvironment in lung cancer: focus on immune checkpoint blockade, Front. Immunol. 12 (2021) 799455, https://doi.org/10.3389/fimmu.2021.799455.Cited in: Pubmed; PMID 35069581.
[7] R. Nooreldeen, H. Bach, Current and future development in lung cancer diagnosis, Int. J. Mol. Sci. 22 (16) (2021), https://doi.org/10.3390/ijms22168661.Cited in: Pubmed; PMID 34445366.
[8] X. Guo, Y. Zhang, L. Zheng, et al., Global characterization of T cells in non-small-cell lung cancer by single-cell sequencing, Nat. Med. 24 (7) (2018) 978–985, https://doi.org/10.1038/s41591-018-0045-3. Cited in: Pubmed; PMID 29942094.
[9] A. Maynard, C. McCoach, J. Rotow, et al., Therapy-induced evolution of human lung cancer revealed by single-cell RNA sequencing, Cell 182 (5) (2020) 1232–1251.e22, https://doi.org/10.1016/j.cell.2020.07.017. Cited in: Pubmed; PMID 32822576.
[10] S. Salcher, G. Sturm, L. Horvath, et al., High-resolution single-cell atlas reveals diversity and plasticity of tissue-resident neutrophils in non-small cell lung cancer, Cancer Cell 40 (12) (2022) 1503–1520.e8, https://doi.org/10.1016/j.ccell.2022.10.008. Cited in: Pubmed; PMID 36368318.
[11] A. Mantovani, P. Allavena, F. Marchesi, C. Garlanda, Macrophages as tools and targets in cancer therapy, Nat. Rev. Drug Discov. 21 (11) (2022) 799–820, https://doi.org/10.1038/s41573-022-00520-5. Cited in: Pubmed; PMID 35974096.
[12] Y. Shu, P. Cheng, Targeting tumor-associated macrophages for cancer immunotherapy, Biochim. Biophys. Acta Rev. Canc 1874 (2) (2020) 188434, https://doi.org/10.1016/j.bbcan.2020.188434.Cited in: Pubmed; PMID 32956767.
[13] M. Pittet, O. Michielin, D. Migliorini, Clinical relevance of tumour-associated macrophages, Nat. Rev. Clin. Oncol. 19 (6) (2022) 402–421, https://doi.org/10.1038/s41571-022-00620-6. Cited in: Pubmed; PMID 35354979.
[14] M. Lavy, V. Gauttier, N. Poirier, S. Barillé-Nion, C. Blanquart, Specialized pro-resolving mediators mitigate cancer-related inflammation: role of tumor-associated macrophages and therapeutic opportunities, Front. Immunol. 12 (2021) 702785, https://doi.org/10.3389/fimmu.2021.702785.Cited in: Pubmed; PMID 34276698.
[15] X. Wang, Y. Xu, Q. Sun, et al., New insights from the single-cell level: tumor associated macrophages heterogeneity and personalized therapy, Biomedicine & pharmacotherapy = Biomedecine & pharmacotherapie 153 (2022) 113343, https://doi.org/10.1016/j.biopha.2022.113343.Cited in: Pubmed; PMID 35785706.
[16] S. Sedighzadeh, A. Khoshbin, S. Razi, M. Keshavarz-Fathi, N. Rezaei, A narrative review of tumor-associated macrophages in lung cancer: regulation of macrophage polarization and therapeutic implications, Transl. Lung Cancer Res. 10 (4) (2021) 1889–1916, https://doi.org/10.21037/tlcr-20-1241. Cited in: Pubmed; PMID 34012800.
[17] I. Larionova, G. Tuguzbaeva, A. Ponomaryova, et al., Tumor-associated macrophages in human breast, colorectal, lung, ovarian and prostate cancers, Front. Oncol. 10 (2020) 566511, https://doi.org/10.3389/fonc.2020.566511.Cited in: Pubmed; PMID 33194645.
[18] L. Liang, H. He, S. Jiang, et al., TIAM2 contributes to osimertinib resistance, cell motility, and tumor-associated macrophage M2-like polarization in lung adenocarcinoma, Int. J. Mol. Sci. 23 (18) (2022), https://doi.org/10.3390/ijms231810415. Cited in: Pubmed; PMID 36142328.
[19] Y. Hao, S. Hao, E. Andersen-Nissen, et al., Integrated analysis of multimodal single-cell data, Cell 184 (13) (2021) 3573–3587.e29, https://doi.org/10.1016/j.cell.2021.04.048. Cited in: Pubmed; PMID 34062119.
[20] C. Trapnell, D. Cacchiarelli, J. Grimsby, et al., The dynamics and regulators of cell fate decisions are revealed by pseudotemporal ordering of single cells, Nat. Biotechnol. 32 (4) (2014 2014/04/01) 381–386, https://doi.org/10.1038/nbt.2859.
[21] D. Witten, R. Tibshirani, Survival analysis with high-dimensional covariates, Stat. Methods Med. Res. 19 (1) (2010) 29–51, https://doi.org/10.1177/0962280209105024.Cited, in: Pubmed; PMID 19654171.
[22] T. Emura, S. Matsui, H. Chen, compound.Cox: univariate feature selection and compound covariate for predicting survival, Comput. Methods Progr. Biomed. 168 (2019) 21–37, https://doi.org/10.1016/j.cmpb.2018.10.020. Cited in: Pubmed; PMID 30527130.
[23] C. Yeh, G. Liao, T. Emura, Sensitivity analysis for survival prognostic prediction with gene selection: a copula method for dependent censoring, Biomedicines 11 (3) (2023), https://doi.org/10.3390/biomedicines11030797.Cited in: Pubmed; PMID 36979776.
[24] Y. Zhou, B. Zhou, L. Pache, et al., Metascape provides a biologist-oriented resource for the analysis of systems-level datasets, Nat. Commun. 10 (1) (2019) 1523, https://doi.org/10.1038/s41467-019-09234-6. Cited in: Pubmed; PMID 30944313.
[25] Z. Tang, C. Li, B. Kang, et al., GEPIA: a web server for cancer and normal gene expression profiling and interactive analyses, Nucleic Acids Res. 45 (2017) W98–W102, https://doi.org/10.1093/nar/gkx247. . Cited in: Pubmed; PMID 28407145.
[26] F. Wu, L. Wang, C. Zhou, Lung cancer in China: current and prospect, Curr. Opin. Oncol. 33 (1) (2021) 40–46, https://doi.org/10.1097/cco.0000000000000703. . Cited in: Pubmed; PMID 33165004.
[27] A. Pallis, K. Syrigos, Lung cancer in never smokers: disease characteristics and risk factors, Crit. Rev. Oncol.-Hematol. 88 (3) (2013) 494–503, https://doi.org/10.1016/j.critrevonc.2013.06.011. Cited in: Pubmed; PMID 23921082.
[28] C. Wang, Q. Yu, T. Song, et al., The heterogeneous immune landscape between lung adenocarcinoma and squamous carcinoma revealed by single-cell RNA sequencing, Signal Transduct. Targeted Ther. 7 (1) (2022) 289, https://doi.org/10.1038/s41392-022-01130-8. Cited in: Pubmed; PMID 36008393.
[29] L. Zhang, Y. Zhang, C. Wang, et al., Integrated single-cell RNA sequencing analysis reveals distinct cellular and transcriptional modules associated with survival in lung cancer, Signal Transduct. Targeted Ther. 7 (1) (2022) 9, https://doi.org/10.1038/s41392-021-00824-9. Cited in: Pubmed; PMID 35027529.
[30] M. Widyananda, V. Kharisma, S. Pratama, et al., Molecular docking study of sea urchin (Arbacia lixula) peptides as multi-target inhibitor for non-small cell lung cancer (NSCLC) associated proteins, Journal of Pharmacy & Pharmacognosy Research 9 (2021 03/15) 484–496.

[31] K. Wei, Z. Ma, F. Yang, et al., M2 macrophage-derived exosomes promote lung adenocarcinoma progression by delivering miR-942, Cancer Lett. 526 (2022) 205–216, https://doi.org/10.1016/j.canlet.2021.10.045. Cited in: Pubmed; PMID 34838826.
[32] J. Chen, K. Zhang, Y. Zhi, et al., Tumor-derived exosomal miR-19b-3p facilitates M2 macrophage polarization and exosomal LINC00273 secretion to promote lung adenocarcinoma metastasis via Hippo pathway, Clin. Transl. Med. 11 (9) (2021) e478, https://doi.org/10.1002/ctm2.478.Cited, in: Pubmed; PMID 34586722.
[33] J. Wu, L. Li, H. Zhang, et al., A risk model developed based on tumor microenvironment predicts overall survival and associates with tumor immunity of patients with lung adenocarcinoma, Oncogene 40 (26) (2021) 4413–4424, https://doi.org/10.1038/s41388-021-01853-y. Cited in: Pubmed; PMID 34108619.
[34] L. Yang, Y. He, S. Dong, et al., Single-cell transcriptome analysis revealed a suppressive tumor immune microenvironment in EGFR mutant lung adenocarcinoma, Journal for immunotherapy of cancer 10 (2) (2022), https://doi.org/10.1136/jitc-2021-003534. Cited in: Pubmed; PMID 35140113.
[35] X. Xiao, Y. Peng, Z. Wang, et al., A novel immune checkpoint siglec-15 antibody inhibits LUAD by modulating mφ polarization in TME, Pharmacol. Res. 181 (2022) 106269, https://doi.org/10.1016/j.phrs.2022.106269.Cited in: Pubmed; PMID 35605813.
[36] L. Santarpia, S. Lippman, A. El-Naggar, Targeting the MAPK-RAS-RAF signaling pathway in cancer therapy, Expert Opin. Ther. Targets 16 (1) (2012) 103–119, https://doi.org/10.1517/14728222.2011.645805.Cited, in: Pubmed; PMID 22239440.
[37] Q. Xu, L. Qin, S. Liang, et al., The expression and potential role of tubulin alpha 1b in wilms' tumor, BioMed Res. Int. 2020 (2020) 9809347, https://doi.org/10.1155/2020/9809347.Cited in: Pubmed; PMID 32908931.
[38] X. Hu, H. Zhu, B. Chen, et al., Tubulin alpha 1b is associated with the immune cell infiltration and the response of HCC patients to immunotherapy, Diagnostics 12 (4) (2022), https://doi.org/10.3390/diagnostics12040858.Cited in: Pubmed; PMID 35453905.
[39] K. Rajkumar, A. Nichita, P. Anoor, et al., Understanding perspectives of signalling mechanisms regulating PEBP1 function, Cell Biochem. Funct. 34 (6) (2016) 394–403, https://doi.org/10.1002/cbf.3198.Cited, in: Pubmed; PMID 27385268.
[40] Y. Xu, Y. Yi, S. Qiu, et al., PEBP1 downregulation is associated to poor prognosis in HCC related to hepatitis B infection, Journal of hepatology 53 (5) (2010) 872–879, https://doi.org/10.1016/j.jhep.2010.05.019. Cited in: Pubmed; PMID 20739083.
[41] Z. Qi, H. Xu, S. Zhang, et al., RIPK4/PEBP1 axis promotes pancreatic cancer cell migration and invasion by activating RAF1/MEK/ERK signaling, Int. J. Oncol. 52 (4) (2018) 1105–1116, https://doi.org/10.3892/ijo.2018.4269.Cited, in: Pubmed; PMID 29436617.